Effects of Phosphonate Ester Groups Attached on a Heteroleptic Ir(III) photosensitizer

Atsushi Kobayashi, Shuhei Watanabe, Masanori Ebina, Masaki Yoshida, Masako Kato**

Department of Chemistry, Faculty of Science, Hokkaido University, North-10 West-8, Kita-ku, Sapporo 060-0810, Japan

*Corresponding authors, e-mail addresses: akoba@sci.hokudai.ac.jp (A.K.), mkato@sci.hokudai.ac.jp (M.K.)

ABSTRACT: Two heteroleptic Ir(III) complexes bearing two diethyl phosphonate groups, $[Ir(ppy\text{-}PE)_2(bpy)](PF_6)$ and $[Ir(ppy)_2(bpy\text{-}dPE)](PF_6)$ (**1pPE** and **1bPE**; Hppy = 2-phenylpyridine, Hppy-PE = 4-(diethylphosphonomethyl)-2-phenylpyridine, bpy = 2,2′-bipyridine, bpy-dPE = 4,4′-bis(diethylphosphonomethyl)-2,2′-bipyridine), were successfully synthesized, and their photophysical properties were investigated by UV–visible absorption and emission spectroscopic and electrochemical measurements. Both **1pPE** and **1bPE** complexes exhibited similar UV–visible absorption and emission spectra and cyclic voltammograms as those of nonmodified complex $[Ir(ppy)_2(bpy)](PF_6)$ (**1**), indicating the suitability for photocatalytic H_2-evolution reaction. ^{3}MLCT emissions of both **1bPE** and **1pPE** were quenched by electron transfer from triethylamine (TEA) sacrificial electron donor, but the quenching rate

of **1pPE** was lower than that of nonmodified complex **1** and **1bPE**. In contrast, the quenching rate of **1bPE** by an electron-accepting $[Co(bpy)_3]^{2+}$ moiety was slightly lower than **1** or **1pPE**. These results suggest that the two diethylphosphonate ester groups regulate the direction of photoinduced electron-transfer reaction at the ^{3}MLCT excited state due to their steric bulkiness. In addition, the photocatalytic activity for H_2 evolution in the presence of K_2PtCl_4 precatalyst clearly showed remarkably extended longevity for both **1pPE** and **1bPE** compared to that of **1**, indicating that the two diethyl phosphonate groups attached on **1pPE** and **1bPE** also play an important role in the extended longevity of H_2-evolution activity of *in-situ*-generated Pt colloidal catalyst from K_2PtCl_4. The deactivation pathway of **1pPE** and **1bPE** during photo H_2 evolution reaction is mainly due to the substitution of the bpy-type ligand by CH_3CN solvent of the one-electron reduced Ir(II) species like the non-substituted complex **1**.

Keywords: Photocatalyst, hydrogen, artificial photosynthesis, cyclometalated Ir(III) complex

Introduction

Solar water-splitting reaction driven by photocatalysts is one of the most attractive reactions to solve global energy issues, because sunlight energy can be converted into the chemical energy of molecular hydrogen (H_2) and oxygen (O_2).[1,2] Considerable efforts have been devoted not only to develop new photocatalysts using semiconductor materials,[3–5] but also to clarify the mechanisms of water-splitting reaction,[6–8] i.e., photoinduced charge separation, water reduction, and water oxidation processes. In this context, photocatalytic systems composed of a molecular photosensitizer and water reduction or oxidation catalyst enable to investigate the reaction steps in more detail than heterogeneous photocatalytic systems such as oxide-based semiconductor

materials. Especially, cyclometalated Ir(III) complexes combined with both homogeneous and heterogeneous catalysts have been reported to exhibit a high catalytic activity for water reduction reaction.[9–18] One of the noteworthy features is that the photocatalytic system does not need any electron-transfer mediators such as methylviologen.[9,10] Such a simple photocatalytic system enables us to investigate the reaction mechanism in more detail than the systems containing electron-transfer mediators. Since the pioneering works by Bernhard and co-workers,[9,10] considerable efforts have been paid to the development of photocatalytic H_2 production systems composed of Ir(III) complexes of diverse homogeneous/heterogeneous catalysts.[9–18]

Recently, several heteroleptic Ir(III) complexes bearing some pendant functional groups on the ligand have been developed to connect the Ir(III) molecular photosensitizer with the heterogeneous metal catalyst.[19–28] A typical example was reported by Bernhard *et al.* involving heteroleptic Ir(III) complexes bearing a vinyl group on the ligand, $[Ir(ppy)_2(mVbpy)]^+$ (Hppy = 2-phenylpyridine, mVbpy = 4-vinyl-4′-methyl-2,2′-bipyridine); the vinyl-functionalized complexes combined with an *in-situ*-generated Pt colloidal catalyst exhibited a better photocatalytic activity, probably because of the effective connection between the molecular Ir(III) photosensitizer and Pt colloidal catalyst.[19] Further, several different functional groups such as pyridyl,[20] nitrile,[21,22] carboxylate,[23–26] and carboxyl ester[27] groups have been introduced on the ppy or bpy ligand; some of them combined with a Pt colloidal catalyst improved the photocatalytic activity. However, a phosphonate and its ester group have been rarely introduced on the ligand of a heteroleptic Ir(III) complex,[27] even though the phosphonate group is well known as a useful functional group to immobilize the molecular photosensitizer on oxide electrodes or nanoparticles (e.g., immobilization of $[Ru(bpy)_3]^{2+}$ moiety on TiO_2 nanoparticles).[29–31] Herein, we report the syntheses, photophysical properties, and photocatalytic

H_2-evolution reaction of luminescent heteroleptic Ir(III) complexes, $[Ir(ppy\text{-}PE)_2(bpy)]PF_6$ and $[Ir(ppy)_2(bpy\text{-}dPE)]PF_6$ (abbreviated as **1pPE** and **1bPE** as shown in Scheme 1; Hppy-PE = 4-(diethylphosphonomethyl)-2-phenylpyridine, bpy = 2,2′-bipyridine, bpy-dPE = 4,4′-bis(diethylphosphonomethyl)-2,2′-bipyridine), bearing two phosphonate ester groups at the ppy or bpy ligand. In this study, we demonstrate that the phosphonate ester groups enhance the longevity of photocatalytic H_2-evolution activity in the presence of an *in-situ*-generated Pt colloidal catalyst, probably because of the weak coordination to the surface of Pt colloid *via* the phosphonate ester groups. The decomposition pathway of these phosphonate-ester-functionalized Ir(III) photosensitizers are also discussed.

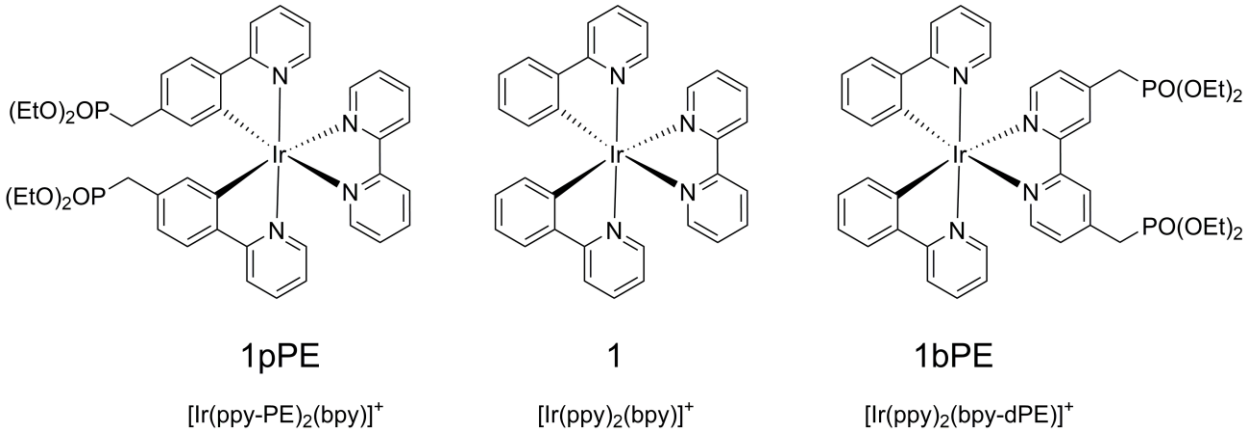

Scheme 1. Molecular structures of complexes **1**, **1pPE**, and **1bPE** used in this study.

Experimental section

Materials and Syntheses

Caution! *Although we had no difficulties, most of the chemicals used in this study are potentially harmful and should be used in small quantities and handled with care in a fume hood.* All the commercially available starting materials were used as received without purification. The starting compounds, bpy-dPE,[32] 4-bromomethyl-2-phenylpyridine (ppy-Br),[33] dichloride-bridged $[Ir(ppy)_2Cl]_2$,[34] nonsubstituted Ir(III) complex, $[Ir(ppy)_2bpy]PF_6$[33], and Co(II) electron relay $[Co(bpy)_3](PF_6)_2$,[10] were prepared following reported procedures. The two heteroleptic Ir(III) complexes, **1pPE** and **1bPE** bearing two diethyl phosphonate groups, were synthesized in moderate yields using a well-known synthetic route with some minor modifications as shown in Scheme 2.

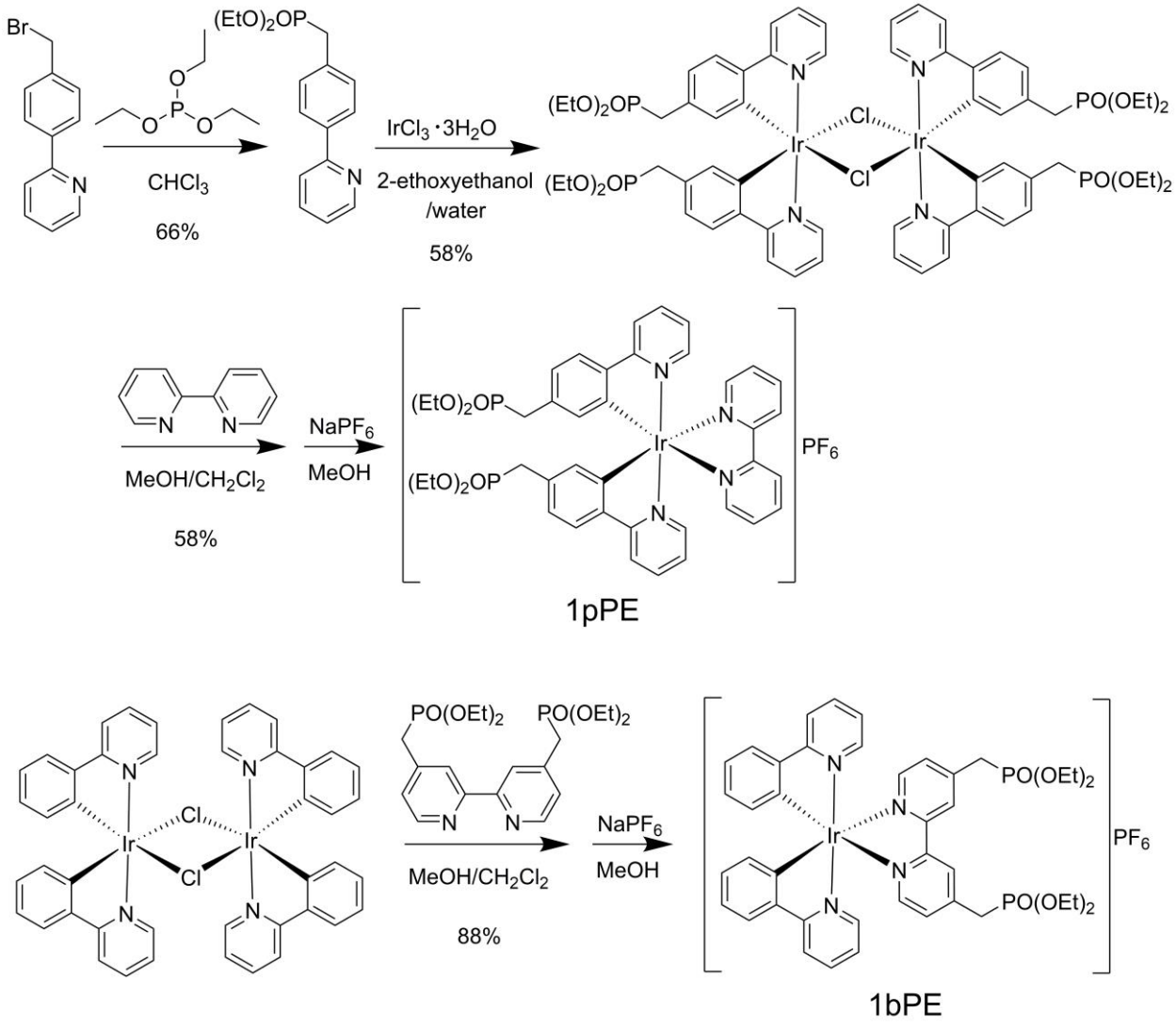

Scheme 2. Synthetic routes for Ir(III) complexes, **1pPE** and **1pPE**, bearing two phosphonate ester groups on the ligand.

ppy-PE

ppy-Br (186 mg, 0.75 mmol) and triethyl phosphite (400 μL, 2.25 mmol) were dissolved in $CHCl_3$ (5 mL), and the mixture was refluxed at 80 °C under N_2 atmosphere for 16 h. The solvent was removed under reduced pressure. The crude product was purified by silica gel column chromatography using a mixture of ethyl acetate/EtOH (9:1 v/v), and the solvent was removed

under reduced pressure, affording ppy-PE as a pale yellow oil. Yield: 144 mg (0.5 mmol, 66%). ^{1}H NMR ($CDCl_3$, 298 K): δ 8.62 (dm, 1H), 7.88 (d, 2H), 7.67 (m, 2H), 7.34 (dd, 2H), 7.15 (m, 1H), 4.01 (q, 4H), 3.14 (d, 2H), 1.19 (t, 6H). Anal. Calcd. (%) for $C_{16}H_{20}NO_3P$: C, 62.94; H, 6.96; N, 4.59. Found: C, 62.60; H, 6.58; N, 4.50.

$[Ir(ppy\text{-}PE)_2Cl]_2$

ppy-PE (678 mg, 2.35 mmol) and $IrCl_3 \cdot 3H_2O$ (243 mg, 0.69 mmol) were added into a mixture of 20 mL 2-ethoxyethanol/water (3:1 v/v); the reaction mixture was heated at 130 °C under N_2 atmosphere for 3 d. The solvent was removed under reduced pressure, and ice-cooled water (40 mL) was added. The yellow precipitate was filtered, affording the target complex $[Ir(ppy\text{-}PE)_2Cl]_2$ as a yellow powder. Yield: 330 mg (0.4 mmol, 58%). ^{1}H NMR ($CDCl_3$, 298 K): δ 9.18 (d, 1H), 7.85 (d, 1H), 7.77 (ddd, 1H), 7.41 (d, 1H), 6.78 (ddd, 1H), 6.73 (td, 1H), 5.72 (s, 1H), 3.68 (m, 4H), 2.73 (dd, 2H), 0.94 (td, 6H). Anal. Calcd. (%) for $C_{64}H_{76}Cl_2Ir_2N_4O_{12}P_4 \cdot 3H_2O$: C, 44.52; H, 4.79; N, 3.24. Found: C, 44.14; H, 4.28; N, 3.27.

$[Ir(ppy\text{-}PE)_2(bpy)]PF_6$ (1pPE)

$[Ir(ppy\text{-}PE)_2Cl]_2$ (87.4 mg, 0.054 mmol) and bpy (19.5 mg, 0.125 mmol) were added into a mixture of 15 mL MeOH/CH_2Cl_2 (1:1 v/v); the mixture was refluxed under N_2 atmosphere for 14 h. The solvent was removed under reduced pressure, affording a yellow powder. The yellow powder was dissolved in a small amount of MeOH, and $NaPF_6$ (100 mg, 0.6 mmol) was added. After stirring at room temperature for 2 h, the yellow precipitate was filtered and washed with a small amount of water for three times. The crude product was recrystallized by the slow liquid-phase diffusion of diethyl ether to a MeOH solution, affording $[Ir(ppy\text{-}PE)_2(bpy)]PF_6$ as an orange-yellow crystalline powder. Yield: 80.9 mg (0.072 mmol, 58%). ^{1}H NMR (DMSO-d_6, 298

K): δ 8.85 (d, 1H), 8.24 (t, 1H), 8.20 (t, 1H), 7.90 (t, 1H), 8.82 (t, 2H), 7.66 (t, 1H), 7.51 (d, 1H), 7.10 (t, 1H), 6.89 (d, 1H), 6.09 (s, 1H), 3.65 (m, 4H), 2.89 (d, 2H), 1.00 (t, 3H), 0.95 (t, 3H). Anal. Calcd. (%) for $C_{42}H_{46}F_6IrN_4O_6P_3 \cdot H_2O$: C, 45.04; H, 4.32; N, 5.00. Found: C, 45.01; H, 3.96; N, 5.01. ESI-TOF MS (CH_3CN, positive): *m*/*z* 957.14 ($[Ir(ppy\text{-}PE)_2(bpy)]^+$).

$[Ir(ppy)_2(bpy\text{-}dPE)]PF_6$ (1bPE)

$[Ir(ppy)_2Cl]_2$ (602 mg, 0.6 mmol) and bpy-dPE (547 mg, 1.2 mmol) were added into a mixture of 100 mL MeOH/CH_2Cl_2 (1:1 v/v); the reaction mixture was refluxed under N_2 atmosphere for 23 h. The solvent was removed under reduced pressure, affording a yellow powder. The yellow powder was dissolved in a small amount of MeOH, and $NaPF_6$ (800 mg, 4.8 mmol) was added. After stirring at room temperature for 2 h, the yellow precipitate was filtered and washed with a small amount of water for three times. The crude product was recrystallized by the slow liquid-phase diffusion of diethyl ether to a MeOH solution, affording $[Ir(ppy)_2(bpy\text{-}dPE)]PF_6$ as an orange-yellow crystalline powder. Yield: 1.172 g (1.06 mmol, 88%). ^{1}H NMR (DMSO-d_6, 298 K): δ 8.68 (s, 1H), 8.27 (d, 1H), 8.20 (t, 1H), 7.94 (t, 2H), 7.78 (d, 1H), 7.60 (t, 2H), 7.15 (t, 1H), 7.02 (t, 1H), 6.90 (t, 1H), 6.20 (d, 1H), 3.95 (m, 4H), 3.55(d, 2H), 1.07 (t, 3H), 1.05 (t, 3H). Anal. Calcd. (%) for $C_{42}H_{46}F_6IrN_4O_6P_3 \cdot H_2O$: C, 45.04; H, 4.32; N, 5.00. Found: C, 44.94; H, 4.01; N, 4.95. ESI-TOF MS (CH_3CN, positive): *m*/*z* 957.24 ($[Ir(ppy)_2(bpy\text{-}dPE)]^+$).

Measurements

Elemental analyses and electrospray ionization time-of-flight (ESI-TOF) mass spectrometry were performed using a MICRO CORDER JM 10 analyzer and JEOL JMS-T100LP

spectrometer, respectively, at the Analysis Center, Hokkaido University. The ^{1}H NMR spectrum of each sample was obtained using a JEOL EX-270 NMR spectrometer at room temperature. UV–visible diffuse reflectance and absorption spectra were obtained using a Shimadzu UV-2400PC spectrophotometer. Luminescence spectra were obtained using a JASCO FP-6600 spectrofluorometer. Quartz cells with a 1-cm optical path length were used for UV–visible absorption and luminescence spectroscopies. The sample solutions were degassed by Ar bubbling for 20 min before the luminescence measurements. Emission quantum yields (Φ_{em}) were measured using a Hamamatsu C9920-02 absolute photoluminescence quantum yield measurement system equipped with an integrating sphere apparatus and a 150-W continuous-wave xenon light source. Emission lifetime measurements were conducted using a Hamamatsu Photonics C4334 system equipped with a streak camera as the photodetector and nitrogen laser as the excitation light source (λ_{ex} = 337 nm). Cyclic voltammetry (CV) was recorded using a HOKUTO DENKO HZ-3000 electrochemical measurement system equipped with glassy carbon, Pt wire, and Ag/AgCl electrodes as the working, counter, and reference electrodes, respectively. A solution of CH_3CN containing 0.1 M tetrabutylammonium hexafluorophosphate ($TBAPF_6$) as the supporting electrolyte and a solution of 2.5 mM Ir(III) complex were used in the CV experiments. All the solutions were deaerated by N_2 bubbling for 30 min before the CV measurements.

Photocatalytic H_2-evolution reactions

For photochemical H_2-evolution reactions, each sample was prepared using a hand-made Schlenk-flask-equipped quartz cell (257 mL in volume). A Pt colloid catalyst protected with polyvinylpyrrolidone (PVP) was synthesized following the published method.[35] Under the dark condition, the Ir(III) complex, triethylamine (TEA), and K_2PtCl_4 or Pt-PVP colloid were added

to the quartz cell as the photosensitizer, sacrificial electron donor, and H_2-evolution catalyst, respectively. The total sample volume was adjusted to 10 mL by adding a mixture of CH_3CN/water (4:1 v/v), where the standard concentrations of the Ir(III) complex, TEA, and Pt used in this study were 1 mM, 0.5 M, and 30 μM, respectively. Each sample flask was doubly sealed using rubber septa and degassed by N_2 bubbling for 30 min. Before the irradiation, gas (0.3 mL) was collected from the headspace using a gas-tight syringe (Hamilton 1001LTN) and analyzed by GC to confirm N_2 purging. Then, the samples were irradiated using a 300-W xenon lamp (MAX-303, ASAHI Spectra) in a water bath combined with a visible-light-passed mirror module (385 nm < λ < 740 nm) at room temperature. The gas samples (0.3 mL) were collected from the headspace at each analysis time for the determination of the amount of H_2 evolved as a function of the irradiation time.

Theoretical Calculations

Density functional theory (DFT) calculations were performed using the B3LYP functional[36] and the LANL2DZ basis[37] set using the Gaussian 03 program.[38] Geometry optimization was achieved using the same functional and basis set. Cartesian coordinates of the optimized structures are shown in Tables S1-3. Visual representation of the molecular orbitals was obtained using the Winmostar V5 program.[39]

Results and Discussion

Photophysical and electrochemical properties

As mentioned in Introduction, cyclometalated Ir(III) complexes are well known to exhibit bright phosphorescence originating from the ^{3}MLCT excited state. To clarify the effect of the introduction of two diethyl phosphonate groups to the ligands (ppy or bpy), UV–visible absorption and emission spectra of the complexes in DMF solutions were measured. Figure 1 shows a comparison of the UV–visible absorption and emission spectra of **1bPE** and **1pPE** with those of nonsubstituted complex **1**. The photophysical data are summarized in Table 1. The nonsubstituted complex **1** has been reported to exhibit singlet ligand-to-ligand charge-transfer (^{1}LLCT) and singlet and triplet metal-to-ligand charge-transfer (^{1}MLCT and ^{3}MLCT) absorption bands at ~370, 405, and 470 nm, respectively.[40–43] Very similar absorption spectra as those of **1** were observed for **1bPE** and **1pPE**, indicating that the introduction of two diethyl phosphonate groups to the ligands hardly affected the electronic absorption property of $[Ir(ppy)_2bpy]^+$ moiety. DFT calculations for these complexes (Figure S1) also indicate that the characteristics of frontier molecular orbitals (MOs) are almost the same as each other, and the two diethyl phosphonate groups did not contribute to these MOs. The DFT calculation for **1** quantitatively agree with the previous reports.[11] The highest occupied molecular orbital (HOMO) is composed of the 5d orbital of Ir atom, and the π orbital is mainly delocalized on the phenyl ring of the cyclometalated ppy ligand. The lowest unoccupied molecular orbitals (LUMOs) of these complexes were localized on the π^* orbital of bpy ligand with a small contribution of the 5d orbital of Ir atom. The HOMO–LUMO energy gaps of the three complexes were also

comparable, ~2.7 eV, consistent with similar UV–visible absorption spectra of the three Ir(III) complexes.

Although similar emission spectra were also observed for these two complexes, a small difference was observed in the emission decay. A ^{3}MLCT phosphorescence band was observed at 609 nm for **1**, and the two functionalized complexes also showed the band at almost the same wavelength with a marginal shift (within 5 nm). The emission quantum yields of the three complexes were also comparable. In contrast, the estimated emission lifetime (Figure S2) of **1pPE** (0.232 μs) was comparable to that of **1** (0.241 μs), whereas a shorter lifetime was observed for **1bPE** (0.177 μs). The radiative and nonradiative rate constants estimated from both the quantum yield and lifetime are shown in Table 1. The k_{nr} of **1bPE** was slightly larger than that of **1** or **1pPE**, indicating that the sterically bulky diethyl phosphonate groups attached on the bpy ligand affect the nonradiative decay process from the ^{3}MLCT emissive state.

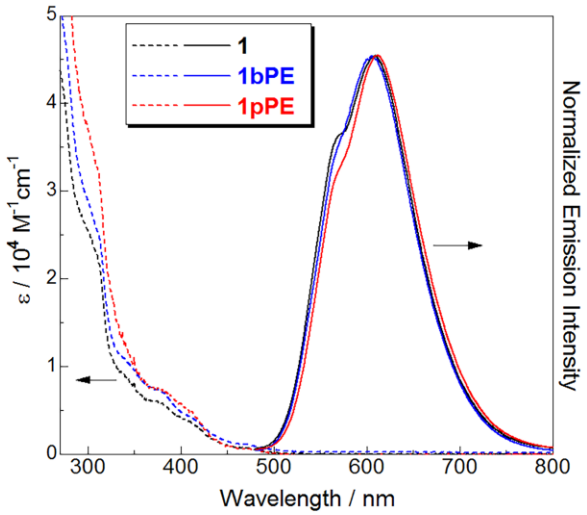

Figure 1. UV–visible absorption (broken lines) and luminescence spectra (solid lines; λ_{ex} = 400 nm) of **1** (black), **1bPE** (blue), and **1pPE** (red) in DMF at 298 K.

Table 1. Photophysical data of three Ir(III) complexes.

Complex	λ_{abs} (nm)	λ_{em} [a] (nm)	τ_{em} [b] (μs)	Φ [c]	k_r [d] (s^{-1})	k_{nr} [e] (s^{-1})
1	375, 405, 470	609	0.241	0.10	4.1×10^5	3.7×10^6
1pPE	380, 410, 473	610	0.232	0.11	4.7×10^5	3.8×10^6
1bPE	376, 405, 467	605	0.177	0.09	5.1×10^5	5.1×10^6

[a] Emission maximum. [b] Emission lifetime. [c] Photoluminescence quantum yields. [d] Radiative rate constants (k_r) were estimated using the equation $\Phi/\tau_{em.}$ [e] Nonradiative rate constants (k_{nr}) were estimated using the equation $k_r(1 - \Phi)/\Phi$.

Figure 2 shows the cyclic voltammograms of the three Ir(III) complexes in a CH_3CN solution. Quasi-reversible oxidation and reduction waves were observed at 1.53 V and −1.14 V, respectively, for the nonsubstituted complex **1**; these were assigned to the oxidation of the Ir center and reduction of the bpy ligand, respectively.[40] As expected from the UV–visible absorption and emission spectroscopic results, similar redox waves were also observed for **1pPE** and **1bPE** at almost the same potentials (within several ten mV shifts), as summarized in Table 2. Thus, the effect of the introduction of the two diethyl phosphonate groups to the ppy or bpy ligand on the ground and excited-state redox property of **1** is negligibly small. In other words, the two complexes **1pPE** and **1bPE** as well as the nonsubstituted complex **1** acted as the redox photosensitizers for H_2 production.

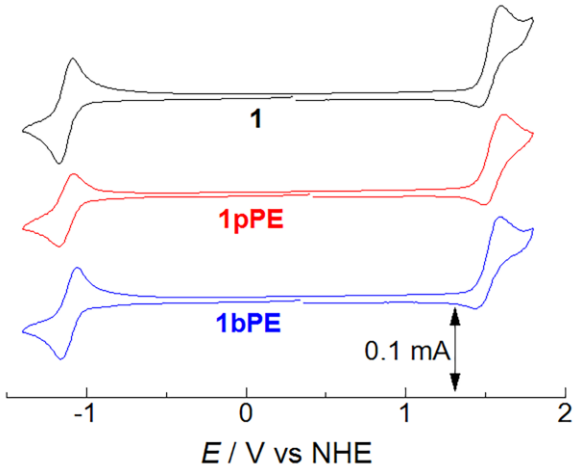

Figure 2. Cyclic voltammograms of 2.5 mM CH_3CN solution of complex **1** (black, top), **1pPE** (red, middle), and **1bPE** (blue, bottom) containing 0.1 M $TBAPF_6$ as the supporting electrolyte and glassy carbon, Pt wire, and Ag/AgCl as the working electrode, counter electrode, and reference electrode, respectively.

Table 2. Ground and excited-state redox properties of the three Ir(III) complexes.

Complex	E_{ox} (V vs NHE)	E_{red} (V vs NHE)	E^*_{ox} (V vs NHE)[a]	E^*_{red} (V vs NHE)[a]
1	1.53	–1.14	–0.51	0.90
1pPE	1.56	–1.13	–0.47	0.90
1bPE	1.52	–1.11	–0.53	0.94

[a] E^*_{ox} and E^*_{red} were estimated using the following equations $E^*_{ox} = E_{ox} - E_{00}$ and $E^*_{red} = E_{red} + E_{00}$, where E_{00} was approximated as λ_{em} (Table 1).

Emission quenching experiments

Luminescence quenching experiments of all the three Ir(III) complexes were conducted using sacrificial electron-donating TEA and electron-accepting $[Co(bpy)_3]^{2+}$ moieties to better understand the effect of the two diethyl phosphonate groups on the photophysical properties of **1pPE** and **1bPE**. Figure 3 shows the Stern–Volmer plots obtained using various concentrations of TEA or $[Co(bpy)_3]^{2+}$. The estimated quenching rate constants are shown in Table 3. In both the cases, the emission of nonsubstituted complex **1** was most effectively quenched by TEA and $[Co(bpy)_3]^{2+}$ than those of **1pPE** and **1bPE**, and the estimated k_q qualitatively agreed with the early report by Bernhard *et al*.[10] Notably, the order of the emission quenching rate of **1bPE** by electron-donating TEA was comparable to that of **1**, whereas that of **1pPE** was smaller by about half of the other two moieties (Figure 3a). In contrast, a completely reverse trend in the emission quenching rate (**1** ≅ **1pPE** > **1bPE**) was observed using the electron-accepting $[Co(bpy)_3]^{2+}$ moiety as the quencher (Figure 3b). These contrasting results indicate that the effect of the two diethyl phosphonate groups on the emission quenching of **1** certainly depends on the position of functionalization. In other words, the two phosphonate groups attached on the ppy ligands (e.g., **1pPE**) suppress the quenching by electron-donating TEA, whereas those attached on the bpy ligand (e.g., **1bPE**) hinder the quenching by $[Co(bpy)_3]^{2+}$. This inverse trend clearly correlates to the HOMO and LUMO of **1**, i.e., the HOMO is mainly localized on both Ir 5d orbital and the phenyl ring of the ppy moiety, whereas the LUMO is localized on the π* orbital of the bpy ligand (Figure S1). Thus, the diethyl phosphonate groups attached on the two ppy ligands would block the access of electron-donating TEA molecules to close to the phenyl ring of **1pPE**, resulting in a smaller quenching rate constant than the other two moieties. Inversely, the diethyl

phosphonate groups on the bpy ligand suppress the emission quenching by electron-accepting $[Co(bpy)_3]^{2+}$ moiety due to their steric bulkiness.

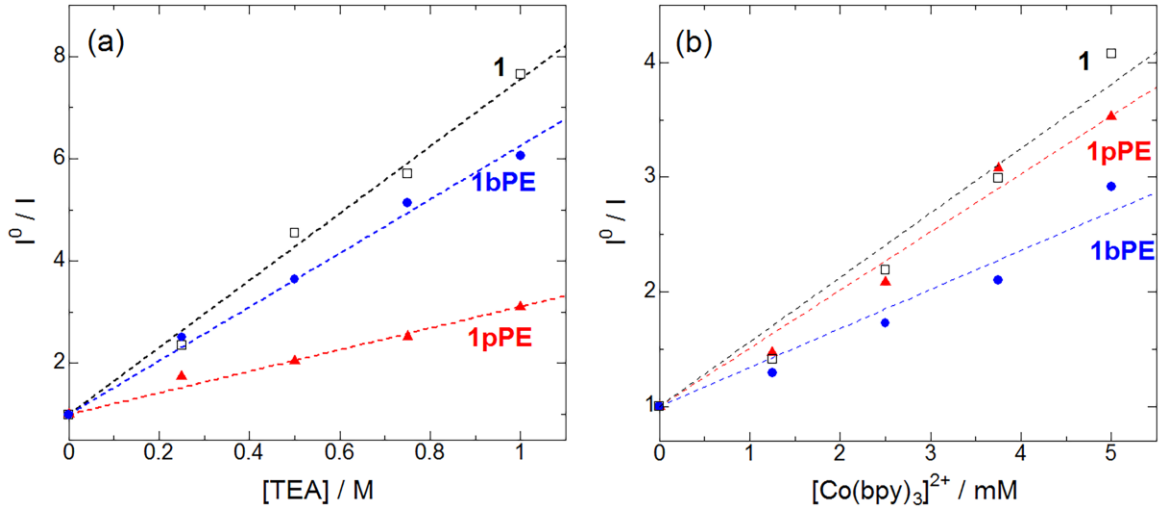

Figure 3. Stern–Volmer plots of **1** (black open square), **1bPE** (blue closed circle), or **1pPE** (red closed triangle) of 1 mM solution in the presence of various concentrations of (a) TEA or (b) $[Co(bpy)_3]^{2+}$ at room temperature. A mixture of CH_3CN/H_2O (4:1 v/v) was used for these measurements.

Table 3. Quenching rate constants of **1**, **1bPE**, and **1pPE** using TEA or $[Co(bpy)_3]^{2+}$.

Complex	TEA		$[Co(bpy)_3]^{2+}$	
	K_{sv} [a]	k_q (s^{-1}) [b]	K_{sv} [a]	k_q (s^{-1}) [b]
1	6.56	2.7×10^7	560	2.3×10^9
1pPE	2.11	9.1×10^6	510	2.2×10^9
1bPE	5.26	3.0×10^7	340	1.9×10^9

[a] Estimated from the slope in the Stern–Volmer plot shown in Figure 3. [b] Estimated using the equation $k_q = K_{SV}/\tau_{em}$. The values of τ_{em} shown in Table 1 were used in this calculation.

Photocatalytic H_2 evolution

As mentioned in previous sections, two Ir(III) complexes with two diethyl phosphonate groups at the ligands, **1bPE** and **1pPE**, exhibited similar photophysical and electrochemical properties as those of the nonsubstituted complex **1**, and the two phosphonate ester groups attached on the ppy and bpy ligands provide a certain effect on the electron-transfer quenching process. To clarify the effect of these functional groups on the photoredox sensitizing ability of the Ir(III) complex, photocatalytic H_2-evolution reaction was investigated in the presence of K_2PtCl_4 as the precatalyst or PVP-protected Pt colloid (Pt-PVP) as the catalyst. These two catalysts have already been reported to evolve H_2 photocatalytically in the presence of **1** as the photosensitizer, and K_2PtCl_4 is reduced with one-electron-reduced Ir(II) species, forming an active Pt colloid catalyst.[11] Figures 4(a) and 4(b) show the results of photocatalytic H_2-evolution reactions in the presence of K_2PtCl_4 precatalyst or Pt-PVP colloid catalyst. The amount of H_2, turnover numbers (TONs), and turnover frequencies (TOFs) are summarized in Table 4. Although only a negligibly small difference was observed in the initial 1-h irradiation in the presence of K_2PtCl_4 precatalyst among the three reaction systems (Figure 4(a) and the initial TOF values shown in Table 4), the photocatalytic activity of the system containing **1** rapidly lost within 2 h. In contrast, the activities of two functionalized complexes **1bPE** and **1pPE** were retained up to 4 h and 6 h, respectively, resulting in larger H_2-evolution amounts than **1**. Considering that the emission quenching rates of **1bPE** and **1pPE** by TEA were comparable and slightly smaller than that of **1**, respectively (see the previous section "Emission quenching experiments"), these extended photocatalytic activities indicate that two diethyl phosphonate groups of **1pPE** and **1bPE** improved the longevity of Ir(III) photosensitizer itself and/or *in-situ*-generated Pt colloid catalyst.

Similar enhanced activities were reported by Bernhard *et al.* for Ir(III) complexes bearing some pendant pyridyl or phenyl groups attached on the bpy ligand.[20]

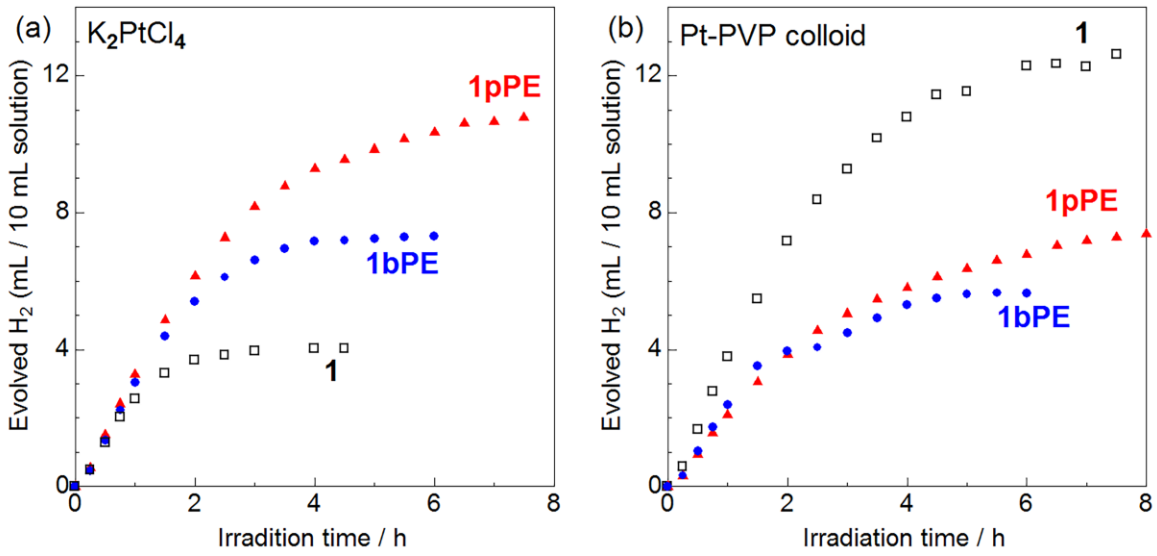

Figure 4. Photocatalytic H_2 evolution of a system containing 1 mM complex **1** (black open square), **1bPE** (blue closed circle), or **1pPE** (red closed triangle) as the photosensitizer, 0.5 M TEA as the sacrificial electron donor in a mixture of CH_3CN/H_2O (4:1 v/v). (a) 30 μM K_2PtCl_4 or (b) Pt-PVP colloid (30 μM as the Pt atom) was used as the H_2-evolution (pre)catalyst.

Table 4. Photocatalytic H_2 evolution using Ir(III) complexes.

Complex	Catalyst	H_2 (μmol)[a]	TON[a,b]	Initial TOF (s^{-1})
1	K_2PtCl_4	4.02	15.5	6.4×10^{-3}
	Pt-PVP colloid	10.79	41.5	9.9×10^{-3}
1pPE	K_2PtCl_4	9.27	35.7	8.4×10^{-3}
	Pt-PVP colloid	5.8	22.3	5.5×10^{-3}
1bPE	K_2PtCl_4	7.16	27.5	7.9×10^{-3}
	Pt-PVP colloid	5.32	20.5	6.4×10^{-3}

[a]After 4-h irradiation. [b]TON = $2n(H_2)/n(Ir)$.

We also investigated the photocatalytic H_2-evolution reaction driven by Pt-PVP colloid catalyst, where the PVP polymer effectively suppressed the Ostwald ripening (growth) of Pt colloid in the dispersed state. Therefore, we assume that the H_2-evolution catalytic activity of the Pt colloid was retained during the reaction. Interestingly, in the presence of Pt-PVP colloid as the H_2-evolution catalyst (Figure 4(b)), the photocatalytic H_2-evolution activity of the system containing **1** was found to be higher than that of **1bPE** or **1pPE** even in the initial 1-h irradiation, and the activity retained up to 6 h was three times longer than the system using K_2PtCl_4 precatalyst. Thus, the shorter longevity of **1** in the presence of K_2PtCl_4 precatalyst can be mainly attributed to the loss of H_2-evolution activity of the *in-situ*-generated Pt colloidal catalyst. The estimated TOFs of **1pPE** and **1bPE** coupled with Pt-PVP colloidal catalyst were less than that obtained with K_2PtCl_4 precatalyst. Because the emission quenching rate of **1bPE** by TEA was comparable to that of **1**, smaller TOFs of these phosphonate-functionalized Ir(III) complexes can be attributed to the slower electron-transfer efficiency from one-electron-reduced Ir(II) species to the Pt-PVP colloidal catalyst, probably because of the sterically bulky phosphonate ester groups of **1pPE** and **1bPE**. Notably, the longevities of the photocatalytic H_2-evolution activities of **1pPE** and **1bPE** seem to be independent of the catalyst. This difference between the reactions driven by the *in-situ*-generated Pt catalyst and Pt-PVP colloidal catalyst indicates that the diethyl phosphonate groups of **1pPE** and **1bPE** improve the catalytic longevity of H_2 evolution of K_2PtCl_4 precatalyst, probably because of the weak coordination of the phosphonate ester groups to the surface of the *in-situ*-generated Pt colloid.[44]

From the view point of the longevity of photocatalytic H_2 evolution activity, the stability of photosensitizing Ir(III) complex is crucial. Therefore, we also investigated the stabilities of these Ir(III) photosensitizers by using several spectroscopic techniques. UV–visible absorption spectral

changes of these three Ir(III) photosensitizers were also measured in the presence of TEA and K_2PtCl_4 precatalyst to determine the stabilities of photosensitizers; all the three Ir(III) complexes gradually and similarly decomposed under light irradiation (Figure S3). In contrast, ^{1}H NMR spectra of these Ir(III) photosensitizers in CD_3CN solution did not changed at all under light irradiation in the absence of sacrificial electron donating TEA (Figure S4), clearly indicating that the decomposition could occur not in the photoexcited state, but in the one-electron reduced Ir(II) state. In fact, similar UV-Vis absorption spectral changes were observed under light irradiation in the absence of K_2PtCl_4 precatalyst (Figure S5) and the ESI-TOF mass spectra of the solutions clearly indicated that the main products are the bpy-ligand-substituted species $[Ir(L)_2(CH_3CN)_2]^+$ (L = ppy or ppy-PE) (Figure S6). In addition, new green emission bands at around 500 nm, which are characteristic of the emission of CH_3CN-bound Ir(III) complexes $[Ir(ppy)_2(CH_3CN)_2]^+$, were clearly observed in these processes (Figure S7),[45] suggesting that the ligand substitution reaction from the bpy ligand to CH_3CN solvent molecules occurs. These spectroscopic data suggest that the major decomposition process of all three Ir(II) complexes could commonly be the ligand substitution from the bpy-type ligand to the CH_3CN solvent molecules in the one-electron reduced Ir(II) states, which was already reported pathway of non-substituted Ir(III) photosensitizer **1**,[11]. Thus, these similar results among three Ir(III) photosensitizers suggest that the photo- and redox-stabilities of $[Ir(ppy)_2(bpy)]^+$ moiety would be hardly affected by the introduction of two phosphonate ester groups at the ppy or bpy ligands.

Conclusion

Two Ir(III) heteroleptic complexes **1pPE** and **1bPE** bearing two diethyl phosphonate groups on the cyclometalated ppy ligand or diimine bpy ligand of a well-known $[Ir(ppy)_2(bpy)]^+$ (**1**) photosensitizer were synthesized, and their photophysical and photosensitizing properties were investigated. The UV–visible absorption and emission spectroscopic and electrochemical measurements showed that the effect of the two phosphonate ester groups on the photophysical properties (e.g., absorption and emission wavelengths and redox potentials) was not obvious, indicating that **1pPE** and **1bPE** complexes as well as the nonmodified complex **1** can act as suitable photoredox sensitizers for H_2 evolution. In the presence of sacrificial TEA electron donor and K_2PtCl_4 precatalyst, both the phosphonate-functionalized complexes exhibited a better photocatalytic performance than **1**, whereas the best photocatalytic performance for **1** was obtained using PVP-protected Pt colloidal catalyst instead of K_2PtCl_4 precatalyst. Emission quenching experiments indicate that the two diethyl phosphonate groups of **1pPE** and **1bPE** moderately regulate the electron-transfer quenching efficiency, probably because of the steric hindrance of these functional groups. Although the phosphonate-ester groups hardly prevent the Ir(III) photosensitizing moiety from the decomposition by the bpy-type ligand substitution, extended longevities of the photocatalytic activities of **1pPE** and **1bPE** obtained using K_2PtCl_4 precatalyst in this study indicate the importance of the interactions between the photosensitizer and H_2-evolving catalyst. Further study on the immobilization of Ir(III) photosensitizer on other metal or oxide substrate *via* the coordination of phosphonate groups is now in progress.

ACKNOWLEDGMENTS

The author (S. W.) thank Mr. H. Kitano (Hokkaido Univ.) for his kind help in the preparation of Pt-PVP colloidal catalyst. This study was supported by JST-PRESTO, Shimadzu Science Foundation, Shorai Science and Technology Foundation, Inamori Foundation, Murata Science Foundation, Grant-in-Aid for Scientific Research (C)(26410063), and Artificial Photosynthesis (No. 2406) from MEXT, Japan.

REFERENCES

[1] M.G. Walter, E.L. Warren, J.R. McKone, S.W. Boettcher, Q. Mi, E.A. Santori, N.S. Lewis, Solar water splitting cells, Chem. Rev. 110 (2010) 6446–6473.

[2] D.L. Ashford, M.K. Gish, A.K. Vannucci, M.K. Brennaman, J.L. Templeton, J.M. Papanikolas, T.J. Meyer, Molecular chromophore−catalyst assemblies for solar fuel applications, Chem. Rev. 115 (2015) 13006–13049.

[3] A. Kudo, Y. Miseki, Heterogeneous photocatalyst materials for water splitting, Chem. Soc. Rev. 38 (2009) 253–278.

[4] K. Maeda, Z‐scheme water splitting using two different semiconductor photocatalysts, ACS Catal. 3 (2013) 1486–1503.

[5] D. Kang, T.W. Kim, S.R. Kubota, A.C. Cardiel, H.G. Cha, K.-S. Choi, Electrochemical synthesis of photoelectrodes and catalysts for use in solar water splitting, Chem. Rev. 115 (2015) 12839–12887.

[6] S. Berardi, S. Drouet, L. Francàs, C. Gimbert-Suriñach, M. Guttentag, C. Richmond, T. Stoll, A. Llobet, Molecular artificial photosynthesis, Chem. Soc. Rev. 43 (2014) 7501–7519.

[7] M.D. Kärkäs, O. Verho, E.V. Johnston, B. Åkermark, Artificial photosynthesis: Molecular systems for catalytic water oxidation, Chem. Rev. 114 (2014) 11863–12001.

[8] L. Duan, L. Wang, F. Li, F. Li, L. Sun, Highly efficient bioinspired molecular Ru water oxidation catalysts with negatively charged backbone ligands, Acc. Chem. Res. 48 (2015) 2084–2096.

[9] M.S. Lowry, J.I. Goldsmith, J.D. Slinker, R. Rohl, R.A. Pascal, G.G. Malliaras, S. Bernhard, Single-layer electroluminescent devices and photoinduced hydrogen production from an ionic iridium(III) complex, Chem. Mater. 17 (2005) 5712–5719.

[10] J.I. Goldsmith, W.R. Hudson, M.S. Lowry, T.H. Anderson, S. Bernhard, Discovery and high-throughput screening of heteroleptic iridium complexes for photoinduced hydrogen production, J. Am. Chem. Soc. 127 (2005) 7502–7510.

[11] L.L. Tinker, N.D. McDaniel, P.N. Curtin, C.K. Smith, M.J. Ireland, S. Bernhard, Visible light induced catalytic water reduction without an electron relay, Chem. Eur. J. 13 (2007) 8726–8732.

[12] F. Gärtner, A. Boddien, E. Barsch, K. Fumio, S. Losse, H. Junge, D. Hollman, A. Brückner, R. Ludwig, M. Beller, Photocatalytic hydrogen generation from water with iron carbonyl phosphine complexes: Improved water reduction catalysts and mechanistic insights, Chem. Eur. J. 17 (2011) 6425–6436.

[13] S. Takizawa, C. Pérez-Bolívar, P. Jr. Anzenbacher, S. Murata, Cationic iridium complexes coordinated with coumarin dyes – Sensitizers for visible-light-driven hydrogen generation, Eur. J. Inorg. Chem. (2012) 3975–3979.

[14] Z.-T. Yu, Y.-J. Yuan, J.-G. Cai, Z.-G. Zou, Charge-neutral amidinate-containing iridium complexes capable of efficient photocatalytic water reduction, Chem. Eur. J. 19 (2013) 1303–1310.

[15] Y.-J. Yuan, Z.-T. Yu, J.-G. Cai, C. Zheng, W. Huang, Z.-G. Zou, Water reduction systems associated with homoleptic cyclometalated iridium complexes of various 2-phenylpyridines, ChemSusChem 6 (2013) 1357–1365.

[16] D.N. Chidron, W.J. Transue, H.N. Kagalwala, A. Kaur, A.B. Maurer, T. Pintauer, S. Bernhard, $[Ir(N^N^N)(C^N)L]^+$: A new family of luminophores combining tunability and enhanced photostability, Inorg. Chem. 53 (2014) 1487–1499.

[17] S.I. Bokarev, D. Hollmann, A. Pazidis, A. Neubauer, J. Radnik, S. Kühn, S. Lochbrunner, H. Junge, M. Beller, A. Brückner, Spin density distribution after electron transfer from triethylamine to an $[Ir(ppy)_2(bpy)]^+$ photosensitizer during photocatalytic water reduction, Phys. Chem. Chem. Phys. 16 (2014) 4789–4796.

[18] S. Takizawa, N. Ikuta, F. Zeng, S. Komaru, S. Sebata, S. Murata, Impact of substituents on excited-state and photosensitizing properties in cationic iridium(III) complexes with ligands of Coumarin 6, Inorg. Chem. 55 (2016) 8723–8735.

[19] S. Metz, S. Bernhard, Robust photocatalytic water reduction with cyclometalated Ir(III) 4-vinyl-2,2′-bipyridine complexes, Chem. Commun. 46 (2010) 7551–7553.

[20] B.F. DiSalle, S. Bernhard, Orchestrated photocatalytic water reduction using surface-adsorbing iridium photosensitizers, J. Am. Chem. Soc. 133 (2011) 11819‑11821.

[21] I.N. Mills, H.N. Kagalwala, D.N. Chirdon, A.C. Brooks, S. Bernhard, New Ir(III) 4,4′-dicyano-2,2′-bipyridine photosensitizers for solar fuel generation, Polyhedron 82 (2014) 104–108.

[22] I.N. Mills, B.S. Kagalwala, Cyano-decorated ligands: A powerful alternative to fluorination for tuning the photochemical properties of cyclometalated Ir(III) Complexes, Dalton Trans. 45 (2016) 10411–10419.

[23] E.I. Mayo, K. Kilså, T. Tirrell, P.I. Djurovich, A. Tamayo, M.E. Thompson, N.S. Lewis, H.B. Gray, Cyclometalated iridium(III)-sensitized titanium dioxide solar cells, Photochem. Photobiol. Sci. 5 (2006) 871–873.

[24] Y.-J. Yuan, J.-Y. Zhang, Z.-T. Yu, J.-Y. Feng, W.-J. Luo, J.-H. Ye, Z.-G. Zou, Impact of ligand modification on hydrogen photogeneration and light-harvesting applications using cyclometalated iridium complexes, Inorg. Chem. 51 (2012) 4123–4133.

[25] Y.-J. Yuan, Z.-T. Yu, X.-J. Liu, J.-G. Cai, Z.-J. Guan, Z.-G. Zou, Hydrogen photogeneration promoted by efficient electron transfer from iridium sensitizers to colloidal MoS_2 catalysts, Sci. Rep. 4 (2014) 4045.

[26] A. Tschierlei, A. Neubauer, N. Rockstroh, M. Karnahl, P. Schwarzbach, H. Junge, M. Bellerd, S. Lochbrunner, Ultrafast excited state dynamics of iridium(III) complexes and their changes upon immobilization onto titanium dioxide layers, Phys. Chem. Chem. Phys. 18 (2016) 10682–10687.

[27] A. Paul, N. Das, Y. Halpin, J.G. Vos, M.T. Pryce, Carboxy derivatised Ir(III) Complexes: Synthesis electrochemistry, photophysical properties and photocatalytic hydrogen generation, Dalton Trans. 44 (2015) 10423–10430.

[28] M. Gennari, F. Légalité, L. Zhang, Y. Pellegrin, E. Blart, J. Fortage, A.M. Brown, A. Deronzier, M.-N. Collomb, M. Boujtita, D. Jacquemin, L. Hammarström, F. Odobel, Long-lived

charge separated state in NiO-based p‐ type dye-sensitized solar cells with simple cyclometalated iridium complexes, J. Phys. Chem. Lett. 5 (2014) 2254–2258.

[29] S.A. Trammell, J.C. Wimbish, F. Odobel, L.A. Gallagher, P.M. Narula, T.J. Meyer, Mechanisms of surface electron transfer. Proton-coupled electron transfer, J. Am. Chem. Soc. 120 (1998) 13248–13249.

[30] M. Haga, K. Kobayashi, K. Terada, Fabrication and functions of surface nanomaterials based on multilayered or nanoarrayed assembly of metal complexes, Coord. Chem. Rev. 251 (2007) 2688–2701.

[31] K. Hanson, D.A. Torelli, A.K. Vannucci, M.K. Brennaman, H. Luo, L. Alibabaei, W. Song, D.L. Ashford, M.R. Norris, C.R.K. Glasson, J.J. Concepcion, T.J. Meyer, Self-assembled bilayer films of ruthenium(II)/polypyridyl complexes through layer-by-layer deposition on nanostructured metal oxides, Angew. Chem. Int. Ed. 51 (2012) 12782–12785.

[32] M.R. Norris, J.J. Concepcion, C.R.K. Glasson, Z. Fang, A.M. Lapides, D.L. Ashford, J.L. Templeton, T.J. Meyer, Synthesis of phosphonic acid derivatized bipyridine ligands and their ruthenium complexes, Inorg. Chem. 52 (2013) 12492–12501.

[33] K.R. Schwartz, R. Chitta, J.N. Bohnsack, D.J. Ceckanowicz, P. Miró, C.J. Cramer, K.R. Mann, Effect of axially projected oligothiophene pendants and nitro-functionalized diimine ligands on the lowest excited state in cationic Ir(III) bis-cyclometalates, Inorg. Chem. 51 (2012) 5082–5094.

[34] S. Sprouse, K.A. King, P.J. Spellane, R.J. Watts, Photophysical effects of metal-carbon σ bonds in ortho-metalated complexes of Ir(II) and Rh(III), J. Am. Chem. Soc. 106 (1984) 6647-6653.

[35] W. Yu, W. Tu, H. Liu, Synthesis of nanoscale platinum colloids by microwave dielectric heating, Langmuir 15 (1998) 6–9.

[36] (a) A.D. Becke, Density-functional thermochemistry. III. The role of exact exchange. J. Chem. Phys. 98 (1993) 5648–5652; (b) C. Lee, W. Yang, R.G. Parr, Development of the Colle-Salvetti correlation-energy formula into a functional of the electron density, Phys. Rev. B 37 (1988) 785–789.

[37] (a) P.J. Hay, W.R. Wadt, Ab initio effective core potentials for molecular calculations. Potentials for the transition metal atoms Sc to Hg. J. Chem. Phys. 82 (1985) 270–283. (b) W.R. Wadt, P.J. Hay, Ab initio effective core potentials for molecular calculations. Potentials for main group elements Na to Bi. J. Chem. Phys. 82 (1985) 284–298. (c) P.J. Hay, W.R. Wadt, Ab initio effective core potentials for molecular calculations. Potentials for K to Au including the outermost core orbitals. J. Chem. Phys. 82 (1985) 299–310.

[38] *Gaussian 03*: Revision E.01, M.J. Frisch, G.W. Trucks, H.B. Schlegel, G.E. Scuseria, M.A. Robb, J.R. Cheeseman, Jr. J.A. Montgomery, J.T. Vreven, K.N. Kudin, J.C. Burant, J.M. Millam, S.S. Iyengar, J. Tomasi, V. Barone, B. Mennucci, M. Cossi, G. Scalmani, N. Rega, G.A. Petersson, H. Nakatsuji, M. Hada, M. Ehara, K. Toyota, R. Fukuda, J. Hasegawa, M. Ishida, T. Nakajima, Y. Honda, O. Kitao, H. Nakai, M. Klene, X. Li, J.E. Knox, H.P. Hratchian, J.B. Cross, C. Adamo, J. Jaramillo, R. Gomperts, R.E. Stratmann, O. Yazyev, A.J. Austin, R. Cammi, C. Pomelli, J.W. Ochterski, P.Y. Ayala, K. Morokuma, G.A. Voth, P. Salvador, J.J. Dannenberg,

V.G. Zakrzewski, S. Dapprich, A.D. Daniels, M.C. Strain, O. Farkas, D.K. Malick, A D. Rabuck, K. Raghavachari, F.B. Foresman, J.V. Ortiz, Q. Cui, A.G. Baboul, S. Clifford, J. Cioslowski, B.B. Stefanov, G. Liu, A. Liashenko, P. Piskorz, I. Komaromi, R.L. Martin, D.J. Fox, T. Keith, M.A. Al-Laham, C.Y. Peng, A. Nanayakkara, M. Challacombe, P.M.W. Gill, B. Johnson, W. Chen, M.W. Wong, C. Gonzalez, J.A. Pople, Gaussian, Inc., Wallingford, CT (2004).

[39] Winmostar V5: N. Senda, Idemitsu-giho, 49 (2006) 106.

[40] K.A. King, R.J. Watts, Dual emission from an ortho-metalated Ir(III) complex, J. Am. Chem. Soc. 109 (1987) 1589–1590.

[41] K. Ichimura, T. Kobayashi, K.A. King, R.J. Watts, Excited-state absorption spectroscopy of ortho-metalated iridium(III) complexes, J. Phys. Chem. 91 (1987) 6104–6106.

[42] A.P. Wilde, K.A. King, R.J. Watts, Resolution and analysis of the components in dual emission of mixed-chelate/ortho-metalated complexes of iridium(III), J. Phys. Chem. 95 (1991) 629–634.

[43] S.-H. Wu, J.-W. Ling, S.-H. Lai, M.-J. Huang, C.H. Cheng, I.-C. Chen, Dynamics of the excited states of $[Ir(ppy)_2bpy]^+$ with triple phosphorescence, J. Phys. Chem. A 114 (2010) 10339–10344.

[44] We cannot rule out a possibility of the contribution of *in-situ*-generated phosphonate groups (not the ester, but the anionic phosphonate) for the coordination to the surface of Pt colloidal catalyst in such a highly basic reaction condition.

[45] B. Schmid, F. O. Garces, R. J. Watts, Synthesis and characterizations of cyclometalated Iridium(III) solvent complexes, Inorg. Chem. 33 (1994) 9–14.